Shallow depth subsurface imaging with microwave holography

Andrei Zhuravlev*[a], Sergey Ivashov[a], Vladimir Razevig[a], Igor Vasiliev[a], Timothy Bechtel[b]
[a]Remote Sensing Laboratory, Bauman Moscow State Technical University, 5 2nd Baumanskaya, Moscow, Russia 105005; [b]Department of Earth and Environment, Franklin & Marshall College, P.O. Box 3003, Lancaster, PA USA 17604-3003

ABSTRACT

In this paper, microwave holography is considered as a tool to obtain high resolution images of shallowly buried objects. Signal acquisition is performed at multiple frequencies on a grid using a two-dimensional mechanical scanner moving a single transceiver over an area of interest in close proximity to the surface. The described FFT-based reconstruction technique is used to obtain a stack of plan view images each using only one selected frequency from the operating waveband of the radar. The extent of a synthetically-formed aperture and the signal wavelength define the plan view resolution, which at sounding frequencies near 7 GHz amounts to 2 cm. The system has a short depth of focus which allows easy selection of proper focusing plane. The small distance from the buried objects to the antenna does not prevent recording of clean images due to multiple reflections (as happens with impulse radars). The description of the system hardware and signal processing technique is illustrated using experiments conducted in dry sand. The microwave images of inert anti-personnel mines are demonstrated as examples. The images allow target discrimination based on the same visually-discernible small features that a human observer would employ. The demonstrated technology shows promise for modification to meet the specific practical needs required for humanitarian demining or in multi-sensor survey systems.

Keywords: Microwave holography, holographic subsurface radar, humanitarian demining, synthetic aperture radar, microwave imaging, automatic data acquisition, linear actuator system.

1. INTRODUCTION

Imaging with microwave holography generally involves two steps: registering both the amplitude and the phase of a wave reflected by a coherently illuminated object over a section of a surface, and establishing the distribution of sources that created the registered distribution of amplitudes and phases. A representation of this distribution may be considered a radar image of the illuminated object. Registration of the reflected signal over an area is frequently achieved with a single microwave transceiver by scanning in two dimensions, with positioning precision and spatial sampling interval being defined based on the wavelength in the medium and the distance to the object. In practical situations, recording of a single microwave hologram for a localized target at frequencies of several Gigahertz requires some hundred samples acquired on a regular grid covering the probing area. Accomplishing this task manually is a tiresome process that rapidly degrades performance of the operator. To address this issue, this paper describes a possible method of automated holographic data acquisition system along with a signal processing technique and data visualization methods. Experimental results using a holographic radar operated in the range of 6.4 – 6.8 GHz are presented to asses plan view resolution of the system.

2. HOLOGRAM REGISTERING AND RECONSTRUCTION

The geometry of sounding with a single transceiver is illustrated by Figure 1, where vector $\boldsymbol{r}$ points to the position of the transceiver and vector $\boldsymbol{r}_0$ gives the position of a hidden point source in the lower half-space $z>0$. If the point source emitted a spherical wave, the distribution of the phase in the plane of sounding would be given by $exp(ik|\boldsymbol{r}-\boldsymbol{r}_0|)$ with its complex conjugate presenting a converging spherical wave at point $\boldsymbol{r}_0$. With the transceiver being the illuminating source the distribution of phase in the interface plane XOY is given by $exp(i2k|\boldsymbol{r}-\boldsymbol{r}_0|)$. The complex conjugate of this distribution gives a converging spherical wave at point $\boldsymbol{r}_0$ with wave number $k'=2k$.

*azhuravlev@rslab.ru; phone/fax 7 495 632-2219; rslab.ru

Detection and Sensing of Mines, Explosive Objects, and Obscured Targets XIX,
edited by Steven S. Bishop, Jason C. Isaacs, Proc. of SPIE Vol. 9072, 90720X
 · doi: 10.1117/12.2051492

With this result in mind, the reconstruction of a microwave hologram may follow the reconstruction principle for optical holograms[1] with the following modification: the complex conjugate of the registered complex amplitude distribution should be propagated back to the medium with the wave number doubled. The following equations formalize the method:

$$\hat{E}(k_x, k_y; 0) = \iint E^*(x, y, 0) e^{-ik_x x} e^{-ik_y y} dxdy \,, \tag{1}$$

$$\hat{E}(k_x, k_y; z) = \hat{E}(k_x, k_y; 0) e^{i\sqrt{(2k)^2 - k_x^2 - k_y^2}\, z} \,, \tag{2}$$

$$E(x, y, z) = \frac{1}{(2\pi)^2} \iint \hat{E}(k_x, k_y, z) e^{ik_x x} e^{ik_y y} dk_x dk_y \,. \tag{3}$$

Equation 1 gives the plane wave decomposition of the complex conjugate to hologram *E(x, y, 0)* registered at interface $z = 0$. Variables x and y are coordinates in a rectangular reference frame connected to the surface. Values k_x and k_y are spatial frequencies with their physical sense of wave vector projections referenced to the coordinate axes. Propagation back to the focusing plane at z is expressed by Equation 2 with the explained doubling of the wave number. This equation is the result of solving the Helmholz equation for complex amplitudes. Equation 3, being the inverse Fourier transform and the result of hologram reconstruction, gives the distribution of sources at depth z parallel to the sounding surface. The Equations 1 – 3 are obtained for a homogeneous media characterized by wave number k.

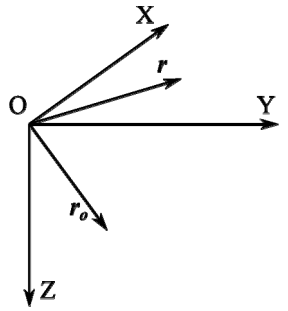

Figure 1. Subsurface sounding geometry.

The reconstruction procedure defined by these equations allows efficient computation using the Fast Fourier Transform (FFT). One of the tested focusing techniques during development of the data processing software consisted of providing the user with the ability to select focusing depth interactively with immediate observation of results. Obtaining the optimum radar image involves interactive selection of proper depth at which the radar image is sharp and small-scale object features are visible. For focusing holograms it was found useful to apply a high pass filter to the spectrum given by Equation 2. The spatial frequencies given by (k_x, k_y) belonging to an area near zero do not provide information on a localized hidden object but rather present a constant or slowly changing reflection from the concealing interface with the changing reflection attributed to possible curvature of this surface.

3. DATA ACQUISITION SYSTEM

The radar system for acquiring microwave holograms consists of an electro-mechanical scanner that carries a continuous wave radar. The scanner consists of two linear actuators with one actuator placed in the carriage of other so that the free carriage of the first one can move in two perpendicular directions. The radar mounts on the free carriage. The completely assembled electro-mechanical scanner is shown in Figure 2. It has adjustable screw legs that can be used to vary the gap between the antenna opening and the surface from 0 to 10 cm. The dimensions of the scanner are 108×100×27 cm with a weight of 15 kg. The maximum scanning area measures 77×84 cm.

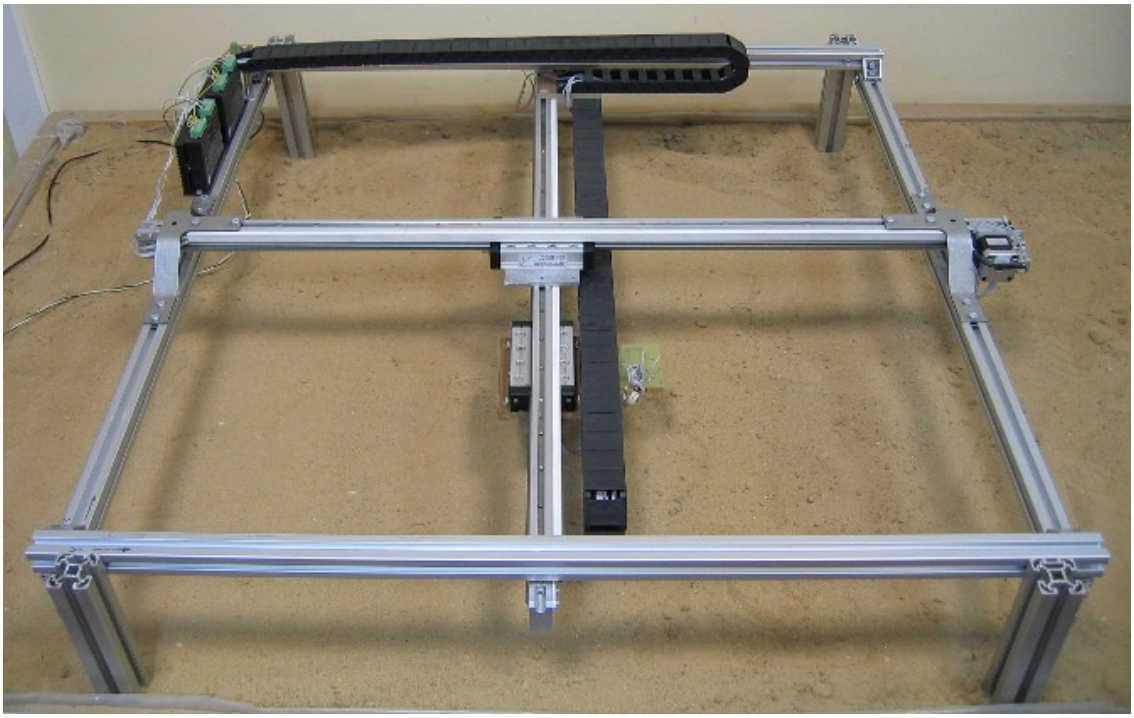

Figure 2. Electro-mechanical scanner for hologram acquisition.

The design of the radar is based on the holographic radar RASCAN[2]. Figure 3 shows the principal electronic diagram of the acquisition system where all controllable by the microcontroller (MCU) items are listed. All the items apart from the MCU board, Bluetooth module and two stepper motor drivers constitute the holographic radar, and are housed in two receiver and transmitter modules that are mounted on the radar antenna as seen in Figure 4. The transmitter consists of a frequency synthesizer clocked by a quartz oscillator at 20 MHz. The synthesizer builds the feedback loop for the voltage-controlled oscillator (VCO) by receiving radio frequency output from the VCO and producing mismatch pulses, which are low-pass filtered, amplified and applied to the VCO as a control voltage. This architecture of the transmitter eliminates phase and frequency drift and allows coherent acquisition of radar data during a prolonged scanning times.

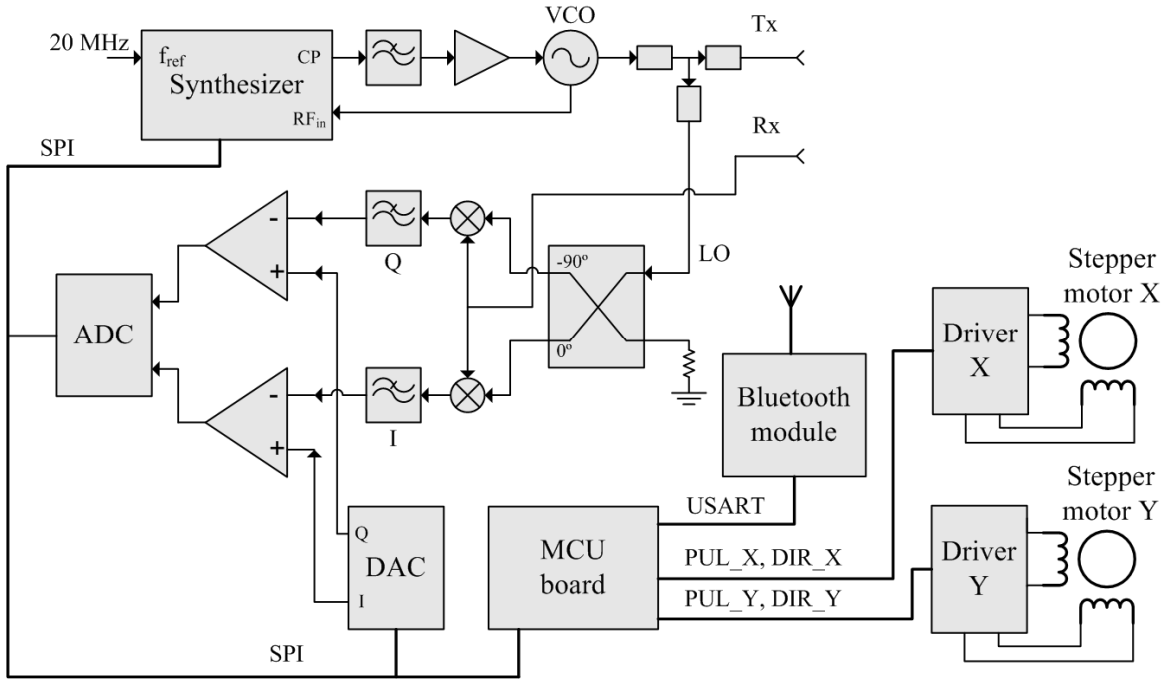

Figure 3. Principal diagram of the data acquisition system with the radar and scanner.

The output of the VCO is split by the directional coupler to provide feed to the antenna and local oscillator input to the mixers. The outputs of the mixers are low-pass filtered and directed to the operational amplifiers whose purpose is to compensate for the signal of constant amplitude caused by strong reflection from the interface. This compensation is usually re-done every time the experimental conditions are changed, i.e. when transitioning to a new surface or changing the gap between the antenna and the sounding surface. The result of the compensation procedure performed by the firmware is a set of coefficients, two for each frequency, which put the analog-to-digital (ADC) output in the middle of its dynamic range. Once compensation is done, a pair of coefficients is applied to the digital-to-analog (DAC) channels every time the radar is switched to the corresponding frequency. The synthesizer, ADC, and DAC are controlled by MCU with Serial Peripheral Interface (SPI), with each of the units having an additional input for addressing (not shown in the figure). A Bluetooth module connected to the microcontroller over Universal Synchronous-Asynchronous Receiver/Transmitter (USART) serves as the data link to the personal computer with user control software.

To move the radar during data acquisition, the MCU board controls two stepper motors through the drivers. The stepper-motor drivers are controlled by MCU logic signals and provide pulses to the motor windings. To control each motor the MCU uses two signals: one sets the direction of movement (DIR), another provides pulses (PUL), each having the effect of rotating the motor for a small preset angle by the positive signal front. Due to the fact that the two motors propel loads of different mass, different pulse frequencies were applied to X and Y drivers, so that the carriage with greater load moves much slower and the rest of the scanner construction does not recoil when the carriage with heavier load starts or stops.

To achieve smooth operation with the scanner the PUL signals are generated inside an interrupt routine that is called by an MCU internal timer event. This timer is especially dedicated to serving stepper-motors and its service routine has the highest execution priority. With such control strategy, the scanner moves and samples continuously without abrupt stops that would result in extraneous vibrations and noise. The side effect of this is that the signal samples taken at adjacent frequencies happen in different places. However, it was found that the displacement of the radar during the full frequency switching cycle was negligibly small compared to a typical sampling interval of 0.5 cm. At the same time, with this sampling interval used in both directions, the acquisition time for a square area with dimensions of 50 cm on a side takes 4 minutes and 50 seconds and can be further decreased.

To derive the linear displacement of the carriage without a gear transfer ratio being provided, a calibration procedure was performed on the drivers. In this procedure a driver is given a known number of pulses followed by the measurement of the carriage displacement. The sensitivity was established after calibration as the number of pulses

required to move the carriage for a given distance unit. This number was stored as a float number in the MCU memory to prevent accumulation of positioning errors during distance calculation at numerous scan lines and sampling positions.

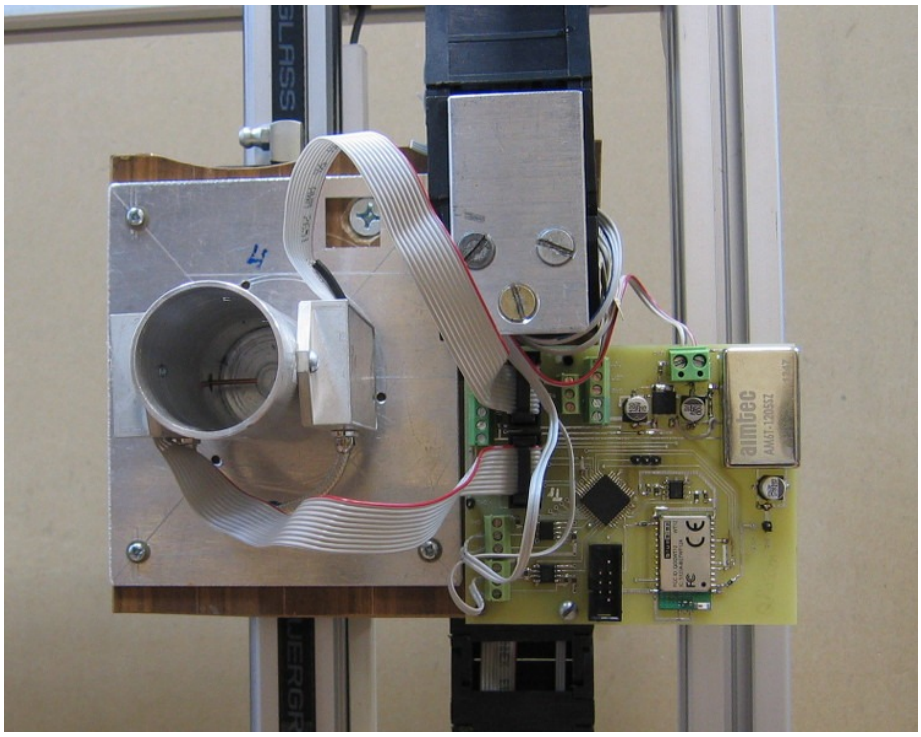

Figure 4. Continuous wave radar for the frequency band 6.4 – 6.8 GHz.

The PC-side software that controls the system allows set-up of data acquisition parameters such as sampling intervals, the size of the scan area, the number of frequencies, and their values. Before scanning, the area the real-time radar signal can be observed as a strip chart to evaluate the necessity for calibrating the radar, which must be done at initial power up. While scanning the area, the display is updated each time a complete line or raster of data is recorded. This helps control the prolonged data acquisition process and to correct it when necessary. On acquiring a microwave hologram, it can be processed with the described technique when the value of dielectric permittivity is set and the depth of focus is found interactively to get the sharpest image. Such images of best focus are presented for objects that were used in the exeriments in the following section. A possible way of finding focusing regions is by presenting vertical slices of the stack of plan view images precalculated with sufficiently small step along axis *Z* so there are no abrupt changes in the resulting image. Figure 5 illustrates the positioning of the cuts in the focusing volume where the sounding plane and the focusing plane are shown, and suggests that the sounding plane coincides with the interface. Two planes, *YZ*-cut and *XZ*-cut dissect the reconstruction volume with point *A* to be selected interactively. Figure 6 gives all the slices depicting distribution of sources for experimental data obtained with a PMN-2 mine as a test object at a frequency of 14.4 GHz, and a distance of 12.4 cm in air. There is the following correspondence among the four images in Figure 6 and the slices shown in Figure 5: *A* – distribution of amplitude of the registered signal at the interface, *B* – focused image at the depth of 12.4 cm, *C* – *YZ*-cut, and *D* – *XZ*-cut of the reconstruction volume. Image *B* in the figure has a photo inset of the mine. As follows from the demonstrated images, the depth of focus is relatively short and allows easy interactive selection of the plane of best focus.

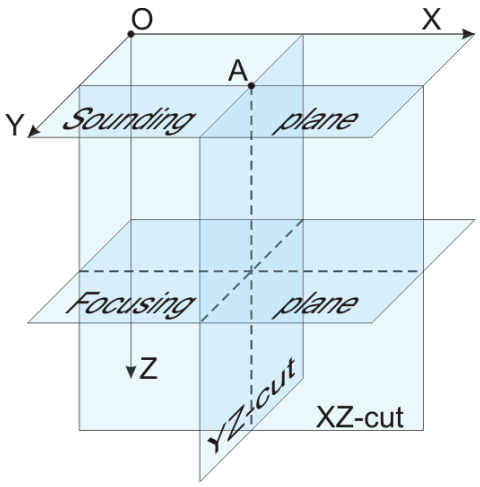

Figure 5. Geometry of sounding with designated sections of reconstructed volume.

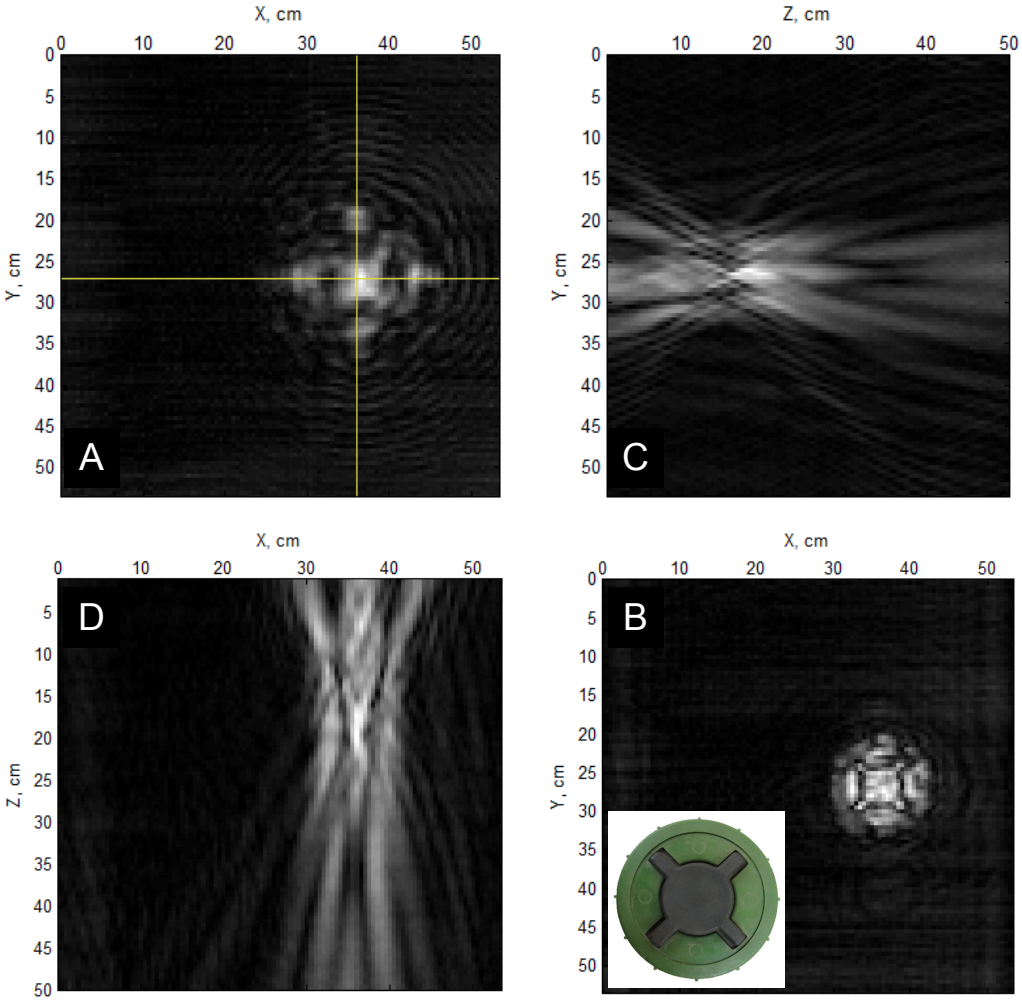

Figure 6. Cuts of reconstructed volume: *A* – amplitude hologram acquired at the interface with intersecting lines being projections of *YZ*- and *XZ*-cut, *B* – the plane of best focus with a photo of the test object, *C* – *YZ*-cut of reconstructed volume, *D* – *XZ*-cut of reconstructed volume.

4. EXPERIMENTAL RESULTS

The experiments with the described data acquisition system were performed in the sandbox with dry sand as seen in Figure 2. Microwave holograms of inert anti-personnel mines and metal reinforcement bars were acquired with the sampling interval of 0.5 cm in both directions at five operating frequencies evenly distributed in the range 6.4 – 6.8 GHz. The typical scanning area measured 50 by 50 cm. The objects selected for the experiments had features of small size above the resolution of the radar system. These features had sufficiently extended flat surfaces considered favorable for the applied reconstruction technique. For every object used in the experiments except for the metal bars, two radar images are demonstrated: when the object was placed on the surface and when it was buried at a shallow depth. The radar image of the object on the surface was obtained to estimate potential resolution of the radar system and compare it to that of the buried object with lesser contrast due to signal loss. The demonstrated images are obtained using the interactive focusing technique described above.

Figure 7 shows an anti-personnel mine PMN-2 that has two different distinctive features: a cross-shaped pressure plate and a T-shaped safety pin on the right side. The radar image of the mine on the surface, acquired from the distance of 9 cm from the top of the mine is shown in the same figure in the middle. Both the pressure plate and the safety pin are distinctly visible. The size of the pressure plate is big enough to reveal its X-shape while the structure of the T-shaped safety pin, having the size of 2.5×2.5 cm, stays beyond the radar resolution at 6.7 GHz. The same mine buried in sand so that the height of the sand layer over its top was 2 cm, as seen in the same figure on the right, has weaker contrast with the safety pin barely visible. The sounding of the buried mine was performed from the distance of 1 cm from the antenna opening to the surface.

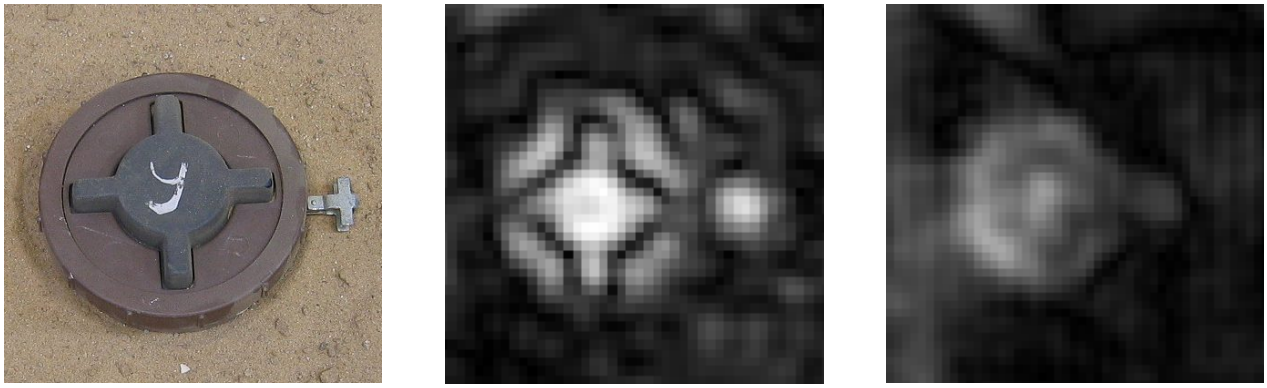

Figure 7. PMN-2 anti-personnel mine: photo (left), radar image of the mine on the surface from the distance of 9 cm (middle), radar image of the mine when it is buried by 2 cm in sand from the distance of 1 cm from the surface (right). The sounding frequency is equal to 6.7 GHz.

The experimental result obtained with an MC-3 antipersonnel mine is found in Figure 8. The optical image of the mine has three distinctive features: a blister in the middle, a filling plug on the left, and a protective cap on the right. On the radar image obtained with the mine on the surface shown in the middle of the same figure only two elements cause significant reflections: the blister in the middle and the protective cap. The latter protects metallic parts of the mine while the filling plug is made entirely of plastic. The same mine, being buried in the sand at the depth of 2 cm, produces a radar image of decreased contrast.

The same behavior exhibits a PFM-1 anti-personnel mine shown in Figure 9 as one of its features, a thin plastic wing, causes no detectable reflection even when mine lies on surface. The other features, the cylindrical fuse well in the center and the container for explosives on the right side, are visible and partly reproduce a visual silhouette of the mine.

An experiment with buried steel reinforcement bars of diameter 16 and 8 mm is shown in Figure 10. The bars were buried at the depth of 2 cm from the surface. The reconstructed radar images were produced by focusing on the upper bars. The plan view resolution does not allow determination of the difference in their sizes. It can be indirectly established by lesser signal reflection from a thinner bar with other parameters being equal.

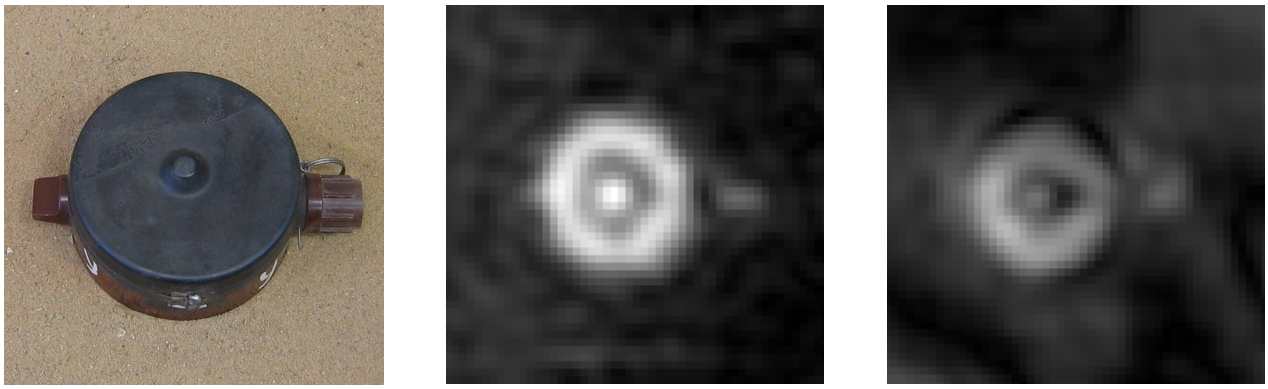

Figure 8. MC-3 anti-personnel mine: photo (left), radar image of the mine on the surface from the distance of 6 cm (middle), radar image of the mine buried by 2 cm in sand from the distance of 2 cm from the surface (right). The sounding frequency is equal to 6.4 GHz.

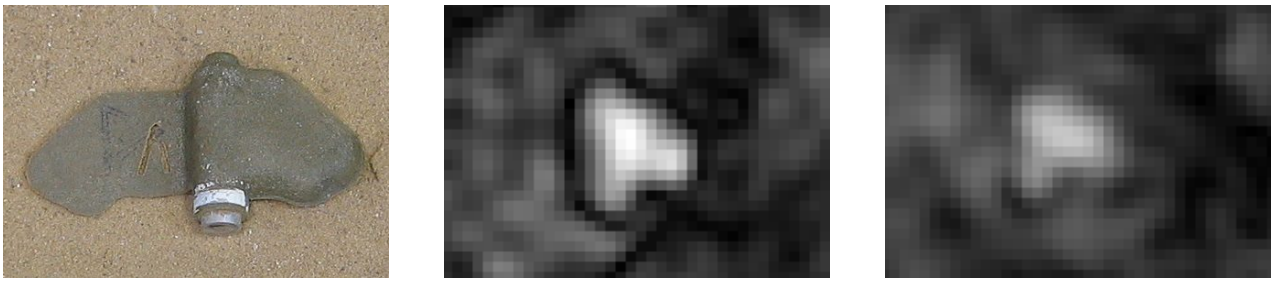

Figure 9. PFM-1 anti-personnel mine: photo (left), radar image of the mine on the surface from the distance of 9 cm (middle), radar image of the mine buried by 1 cm in sand from the distance of 3 cm from the surface (right). The sounding frequency is equal to 6.4 GHz.

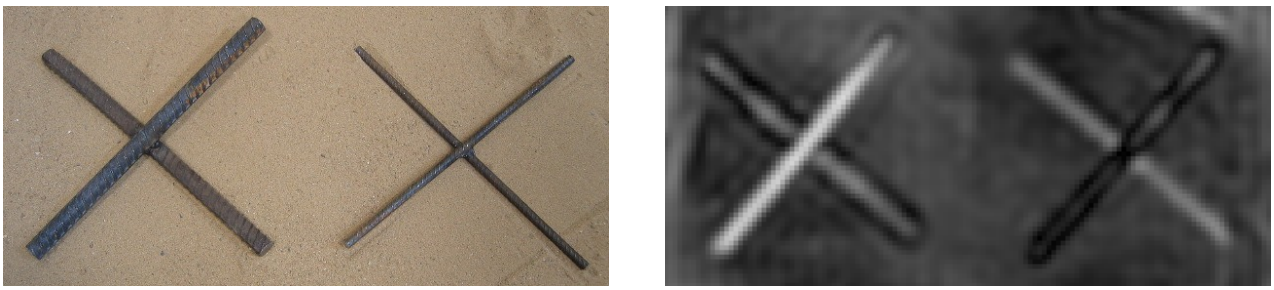

Figure 10. Metal reinforcement bars with the diameters 16 and 8 mm: photo (left), radar image of the bars buried by 2 cm in sand from the distance of 1 cm from the surface (right).

5. CONCLUSION AND FUTURE WORK

Microwave holography is shown in the paper to have the ability to produce high resolution images of objects at shallow depths. This is achieved by high sensitivity of the radar system to the phase of the received signal and extensive synthetic aperture that give images with short depth of focus. Due to this, small changes in the relief of the localized objects produce sufficient contrast. The automated data acquisition system substantially increases the productivity of hologram acquisition compared to manual acquisition and makes it possible over uneven surfaces without direct contact. It can be modified to be used with other types of sensors.

One possible way of enhancing the system is increasing the bandwidth of the radar. A modified signal processing technique can then produce radar images whose depth of focus will be additionally reduced by the increased bandwidth in addition to the effect that gives synthetic aperture.

ACKNOWLEDGEMENT

This work is supported by Russian Foundation for Basic Research.

The first author is very grateful to Dr. Timothy Bechtel and Enviroscan, Inc. for forwarding the invitation letter from SPIE by fast courier service, so that the author could apply for and get a travel visa in proper time and participate in the conference.

REFERENCES

[1] Goodman J.V., [Introduction to Fourier Optics], McGraw-Hill, New York, (2005).
[2] Zhuravlev A.V., Ivashov S.I., Razevig V.V., Vasiliev I.A., Bugaev A.S., "Holographic subsurface radar RASCAN-5," 7th International Workshop on Advanced Ground Penetrating Radar (IWAGPR), 2-5 July 2013.